

# International Journal of Pharmacology

ISSN 1811-7775





ISSN 1811-7775 DOI: 10.3923/ijp.2023.52.63



# Research Article Potential Targets and Mechanisms of *Dalbergia odorifera* on Treating Lung Adenocarcinoma Explored by Network Pharmacology

Zhongyv Xiong and Yan Wang

Key Laboratory of Tropical Translational Medicine of Ministry of Education,
Hainan Provincial Key Laboratory for Research and Development of Tropical Herbs,
Haikou Key Laboratory of Li Nationality Medicine, School of Pharmacy, Hainan Medical University, Haikou 571199, China

# **Abstract**

**Background and Objective:** *Dalbergia odorifera* (DO) is a medicinally important plant which showed anticancer effects in osteosarcoma and neuroblastoma, however, it lacks data on Lung Adenocarcinoma (LUAD). Therefore, the effect of DO on LUAD was explored in this study. **Materials and Methods:** The main active components of DO, targets of DO and LUAD disease targets were obtained from databases including the TCMSP and Gene Cards. While, the top 10 hub targets of overlapping genes were analyzed by the topological structure (CytoNCA), Molecular Complex Deletion (MCODE) plugin and cytoHubba. Moreover, the correlation between hub gene expression and LUAD was confirmed on the Gene Expression Profiling Interactive Analysis Dataset (GEPIA). **Results:** A total of 37 core active components were selected according to the screening criteria of ADME OB≥30% and DL≥0.18. While 627 genes overlapped between targets of DO and LUAD, of which STAT3, EGFR, SRC, PTK2, PTPN11, MAPK1, LYN, LCK, CTNNB1 and MAPK3 were defined as the hub genes involved in the anti-LUAD effects of DO. Moreover, the mRNA expression of LCK is associated with the prognosis stages and median survival time of LUAD. **Conclusion:** The application of network pharmacology analysis provides a theoretical mechanism for the pharmacological effect of DO against LUAD.

Key words: Dalbergia odorifera, lung adenocarcinoma, network pharmacology, osteosarcoma cell, proto-oncogene, target fishing, gene expression

Citation: Xiong, Z. and Y. Wang, 2023. Potential targets and mechanisms of *Dalbergia odorifera* on treating lung adenocarcinoma explored by network pharmacology. Int. J. Pharmacol., 19: 52-63.

Corresponding Author: Yan Wang, Key Laboratory of Tropical Translational Medicine of Ministry of Education, Hainan Provincial Key Laboratory for Research and Development of Tropical Herbs, Haikou Key Laboratory of Li Nationality Medicine, School of Pharmacy, Hainan Medical University, Haikou 571199, China

Copyright: © 2023 Zhongyv Xiong and Yan Wang. This is an open access article distributed under the terms of the creative commons attribution License, which permits unrestricted use, distribution and reproduction in any medium, provided the original author and source are credited.

Competing Interest: The authors have declared that no competing interest exists.

Data Availability: All relevant data are within the paper and its supporting information files.

# **INTRODUCTION**

Lung cancer is the leading cause of cancer-related death with an increasing burden globally<sup>1</sup>, of which, 75-80% is Non-Small Cell Lung Cancer (NSCLC)<sup>2,3</sup>. According to the classification of World Health Organization, NSCLC is generally subcategorized into adenocarcinoma (LUAD), squamous cell carcinoma and large cell carcinoma<sup>4,5</sup>, the former is the main subtype comprising nearly 50% of all lung cancer cases<sup>6</sup>.

Up to date, drugs targeted to epidermal growth factor receptor (EGFR)<sup>7</sup>, Anaplastic Lymphoma Kinase (ALK)<sup>8-13</sup> and ROS1 Proto-Oncogene (ROS1)<sup>14</sup> have been proven to improve the therapeutic efficacy of LUAD<sup>15</sup>. However, the treatment has a marginal effect on certain types of LUAD. Few patients can escape drug resistance<sup>16</sup>. Recent data revealed that half of LUAD patients die within one year after diagnosis and the five years survival rate is below 20%, evenly<sup>17</sup>. Therefore, exploring new drug therapy for LUAD is still emergent.

Dalbergia odorifera T. Chen (DO) is a medicinally important plant mainly found in China. Traditionally, heartwood is used to treat blood disorders, ischemia<sup>18</sup>, swelling and rheumatic pain in China and Korea. Recently, compounds isolated from DO show anticancer properties. In detail, 4-parvifuran inhibited metastatic and invasive actions on osteosarcoma cells<sup>19</sup>. Besides, cearoin was shown to prevent neuroblastoma cells from ROS-induced apoptosis<sup>20</sup>. Moreover, fisetin extracted from the root of DO could inhibit MMP-1, MMP-3, MMP-7 and MMP-9 and reduce tumour cell invasiveness<sup>21</sup>. However, the effects of DO on LUAD have never been reported.

Network pharmacology of traditional Chinese medicine (TCM), which is based on high-throughput data analysis and virtual computing and integrated bio-information network construction with network topology analysis strategy<sup>22</sup>, is widely used to dissect active ingredients in the classical TCM prescription and single herb. Therefore, in the present study, the potential compounds and targets of DO were employed on LUAD via network-based pharmacological methods.

## **MATERIALS AND METHODS**

**Study area:** This study was carried out in the School of Pharmacy, Hainan Medical University, Haikou, China, from January to November, of 2021.

**Exploration of the main active ingredients of DO:** The traditional Chinese medicine system pharmacology database and analysis platform (TCMSP, https://tcmspw.com

/tcmsp.php) were applied to identify the active ingredients of DO. According to the optimal toxicokinetic ADME rules reported in the literature, compounds with OB≥30% and DL≥0.18 were selected as the main active ingredients. Then, the relative compounds were input into PubChem (https://pubchem.ncbi.nlm.nih.gov/) to obtain the molecular structure.

**Potential targets of DO:** Information on the small molecule structure of the core active ingredient (Canonical SMILES) was used to identify potential targets via the Similarity ensemble approach (https://sea.bkslab.org/) and Swiss Target Prediction (https://new.swisstargetprediction.ch/) websites.

**Achievement of LUAD-related targets:** The target genes of LUAD were collected from Gene Cards (https://www.genecards.org/, version 4.9.0), which is a database integration with genome, transcriptome, proteome and genetics, as well as clinical and functional information from 150 web sources.

# Construction of a "herbs components targets" network:

Overlapping targets between core active ingredients of DO and LUAD were visualized by a VENN map drawn by Bioinformatics (https://bioinformatics.psb.ugent.be /webtools/Venn/). Then, the protein-protein interaction (PPI) network of the overlapping targets was obtained through the STRING online tool (https://string-db.org/). Core genes were analyzed by the plugin (CytoNCA) of Cytoscape 3.6.1 (https://www.cytoscape.org/). Three parameters including the degree of degree centrality (DC), closeness centrality (CC) and betweenness centrality (BC) were selected to screen the core composite targets<sup>23</sup>. The DC refers to the number of other nodes associated with a node in the network, while, BC and CC represent the number of shortest paths through a node and the sum of the distances from one point to all other points, respectively. According to relevant literature reports, the target with a twofold median value for DC and median value for BC and CC was selected to obtain more accurate core targets.

**Network module analysis:** The Molecular Complex Deletion (MCODE) plugin for Cytoscape was used to cluster the network modules (37). Densely connected regions or clusters in the coexpression network were identified using the following parameters:

- Degree cut-off = 2
- k-core = 2
- max. depth = 100

**Gene functions and pathway:** Geno ontology (GO) gene functions and biochemical pathways enriched by the core targets were determined by using the web-based annotation tool DAVID v6.8 (https://david.ncifcrf.gov/tools.jsp), providing GO terms in the categories biological process (BP), cellular component (CC), molecular function (MF), Kyoto Encyclopedia of Genes and Genomes pathways (KEGG). The p<0.05 was used as the significance threshold.

# Correlation analysis between hub gene expression and

**LUAD:** The top 10 hub genes were verified by the plugin (cytoHubba) of Cytoscape, in which "MCC" was applied to calculate and the "display the shortest path" was selected to display. Moreover, the Gene Expression Profiling Interactive Analysis dataset (GEPIA, http://gepia.cancer-pku.cn/) was used to analyze the differentiated expression,

pathological stages and overall survival of hub genes between LUAD and normal tissues. log 2 FC cutoff = 1, q value cutoff = 0.05, while the other options were set as the default values.

#### **RESULTS**

**Potential ingredients and predicted targets of DO:** A total of 87 active ingredients were obtained from TSMSP, of which 37 ingredients with the screening criteria of ADME OB≥30% and DL≥0.18 were defined as the core active components (Table 1). Based on the Canonical SMILES number of core active ingredients of DO, 796 genes were predicted by target fishing and integrating the data obtained from SEA and SWISS, of which 627 targets were matched with that of LUAD (Fig. 1).

Table 1: Information of DO ingredients with OB > 30% and DL > 0.18

Mol. ID	Name	OB (%)	DL
MOL001040	(2R)-5,7-dihydroxy-2-(4-hydroxyphenyl)chroman-4-one	42.36	0.21
MOL001792	DFV	32.76	0.18
MOL000228	(2R)-7-hydroxy-5-methoxy-2-phenylchroman-4-one	55.23	0.20
MOL002565	Medicarpin	49.22	0.34
MOL002914	Eriodyctiol (flavanone)	41.35	0.24
MOL002938	(3R)-4'-Methoxy-2',3,7-trihydroxyisoflavanone	68.86	0.27
MOL002939	(3R)-5'-Methoxyvestitol	83.06	0.26
MOL002940	(3R)-3-(2,3-dihydroxy-4-methoxyphenyl)-7-hydroxychroman-4-one	52.06	0.27
MOL002941	(3R)-3-(2,3-dihydroxy-4-methoxyphenyl)chroman-7,8-diol	82.35	0.27
MOL002950	(3R)-7,2',3'-trihydroxy-4-methoxyisoflavan	69.65	0.24
MOL002957	9-O-Methylcoumestrol	33.73	0.38
MOL002958	3'-Hydroxymelanettin	30.69	0.27
MOL002959	3'-Methoxydaidzein	48.57	0.24
MOL002961	(-)-Vestitol	70.29	0.21
MOL002962	(3S)-7-hydroxy-3-(2,3,4-trimethoxyphenyl)chroman-4-one	48.23	0.33
MOL002963	4',5',7-trimethyl-3-methoxyflavone	40.66	0.25
MOL002966	Dalbergin	78.18	0.20
MOL002967	7-hydroxy-4'-methoxy-2',5'-dioxo-4-[(3R)-2',7-dihydroxy-4'-methoxyisoflavan-5'-yl]isoflavane	34.78	0.70
MOL002973	Bowdichione	55.78	0.28
MOL002975	butin	69.94	0.21
MOL002981	Duartin	70.63	0.34
MOL002982	(3R,4R)-3',7-dihydroxy-2',4'-dimethoxy-4-[(2S)-4',5,7-trihydroxyflavanone-6-yl]isoflavan	33.96	0.63
MOL002985	isoduartin	74.11	0.34
MOL002989	4-Hydroxyhomopterocarpin	48.41	0.43
MOL002990	(6aR,11aR)-3,9,10-trimethoxy-6a,11a-dihydro-6H-benzofurano[3,2-c]chromen-4-ol	66.86	0.53
MOL002991	(6aR,11aR)-3,9-dimethoxy-6a,11a-dihydro-6H-benzofurano[3,2-c]chromene-4,10-diol	38.96	0.48
MOL002996	odoricarpin	55.02	0.53
MOL002997	3-(2-hydroxy-3,4-dimethoxyphenyl)-2H-chromen-7-ol	86.18	0.27
MOL002999	Sativanone	85.63	0.27
MOL003000	Stevein	36.54	0.24
MOL003001	Vestitone	52.83	0.24
MOL003002	violanone	80.24	0.30
MOL003003	Xenognosin B	72.71	0.24
MOL000358	beta-sitosterol	36.91	0.75
MOL000359	sitosterol	36.91	0.75
MOL000380	(6aR,11aR)-9,10-dimethoxy-6a,11a-dihydro-6H-benzofurano[3,2-c]chromen-3-ol	64.26	0.42
MOL000392	formononetin	69.67	0.21

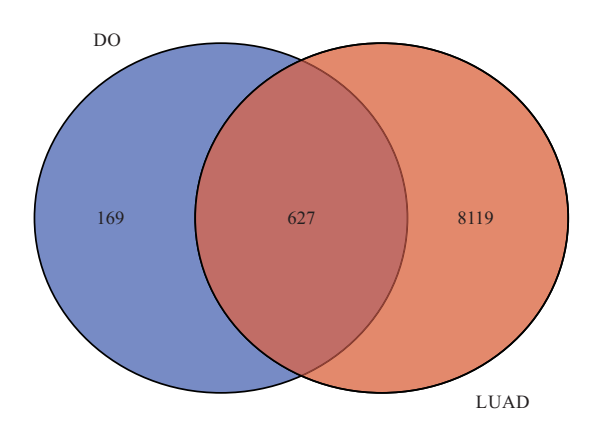


Fig. 1: Overlapping genes between DO and LUAD

A total of 796 targets of DO was predicted by the Swiss and CEA database, while 8746 genes closely associated with LUAD were extracted from the website of Gene Cards. Overall, the Venn diagram figured 627 overlapping genes including between DO and LUAD

Herbs-components-targets network of DO and module identification: Those overlapping targets (627) were input into STRING to remove the unconnected target (combined score <0.7) and constructed a PPI network. It showed that the network contained 579 nodes and 4565 edges (Fig. 2a), of which 63 of core targets including EGFR, Phosphatidylinositol-4,5-Bisphosphate 3-Kinase Catalytic Subunit Alpha (PIK3CA) and Catenin beta 1 (CTNNB1) were retrieved with the cutoff of DC (31.5), BC (1149.9) and CC (0.20) (Fig. 2b). The 63 core targets covered three modules in which module 1 contained 219 edges with 30 nodes (Fig. 2c), module 2 included 50 edges with 11 nodes (Fig. 2d), module 3 contained 34 edges with 15 nodes (Fig. 2e).

**GO and KEGG enrichment analysis:** The GO and pathways enrichment analysis was performed for the 63 core targets, which were significantly enriched on signal transduction, positive regulation of transcription from RNA polymerase II promoter and negative regulation of apoptotic process in the BP. In terms of CC, it was enriched on the nucleus, cytoplasm and cytosol. Concerning the MF, those core targets were enriched on protein binding, ATP binding and enzyme binding (Fig. 3). Besides, pathways in cancer, proteoglycans pathway and PI3K-AKT signalling pathway were the most concentrated pathways (Fig. 4).

# Hub genes analysis and differentiated expression in LUAD:

The top 10 hub genes were explored by plugin cytoHubba, which included Signal Transducer and Activator of Transcription 3 (STAT3), EGFR, SRC, Mitogen-Activated Protein

Kinase 3 (MAPK3), Protein Tyrosine Kinase 2 (PTK2), MAPK1, Protein Tyrosine Phosphatase Non-Receptor Type 11 (PTPN11), Lymphocyte-specific protein tyrosine kinase (LCK), LYN and CTNNB (Fig. 5). There was no change for other genes (Fig. 6a-i), however, slightly decreased expression of LCK was shown in LUAD tissue, compared with that of normal tissue (Fig. 6j), Moreover, mRNA expression of STAT3, EGFR, SRC, MAPK3, PTK2, MAPK1, PTPN11, LYN and CTNNB did not associate with prognosis stages of LUAD (Fig. 7a-i). However, a negative correlation was shown between mRNA expression of LCK and prognosis stages of LUAD (Fig. 7h). Similarity, expression of STAT3, EGFR, SRC, MAPK3, PTK2, MAPK1, PTPN11, LYN and CTNNB did not relate to the median survival time (Fig. 8a-i). However, the median survival time of a low-expression group of LCK was lower than that of a highexpression group (Fig. 8i).

## **DISCUSSION**

Dalbergia odorifera T. Chen is indigenous to Hainan Province in South China. The history of DO use in China begins in the description of the ancient Chinese medical book "Hai Yao Ben Cao" (Tang and Five Dynasties, late 9th century to mid-10th century)<sup>24</sup>. To date, DO has been used in more than 100 TCM prescriptions including Qi Shen Yi Qi (QSYQ) pills and Tongxinluo capsules for the treatment of coronary heart and cerebrovascular diseases<sup>25</sup>.

A total of 175 chemical constituents have been isolated from the heartwood, roots, leaves and seeds of DO, including flavonoids, aryl benzofurans, phenols and guinones<sup>24</sup>. While the pharmacological effects varied among those compounds. Overall, flavonoids were shown to be the anti-inflammatory compounds in DO. Isoflavones could inhibit nitric oxide production in RAW 264.7 macrophages<sup>26</sup>. Also, isoliquiritigenin and 4,2'5'-trihydroxy-4'-methoxychalcone exerted an antiinflammatory effect by upregulating the expression of heme oxygenase-1 through Nrf-2<sup>27,28</sup>. In terms of benzofuran, isoparvifuran showed antisenescence effects<sup>29</sup>, while aryl benzofuran could suppress neuroinflammation in microglial and hippocampal HT22 cells<sup>30</sup>. Another major compound (volatile oil) was shown to owe cardiac-protection effects<sup>31</sup> and affected the metabolome of chronic myocardial ischemic pigs, including energy, glucose and fatty acid metabolism when combined with Salvia miltiorrhiza<sup>32</sup>. Besides, the volatile oil of DO increased the absorbance of major ingredients in QSYQ<sup>33</sup>. Recently, latifolin, as a newly extracted flavonoid, was shown to protect against myocardial infarction and oxidative stress-induced senescence<sup>34,35</sup>. The 6,4'-Dihydroxy-7-

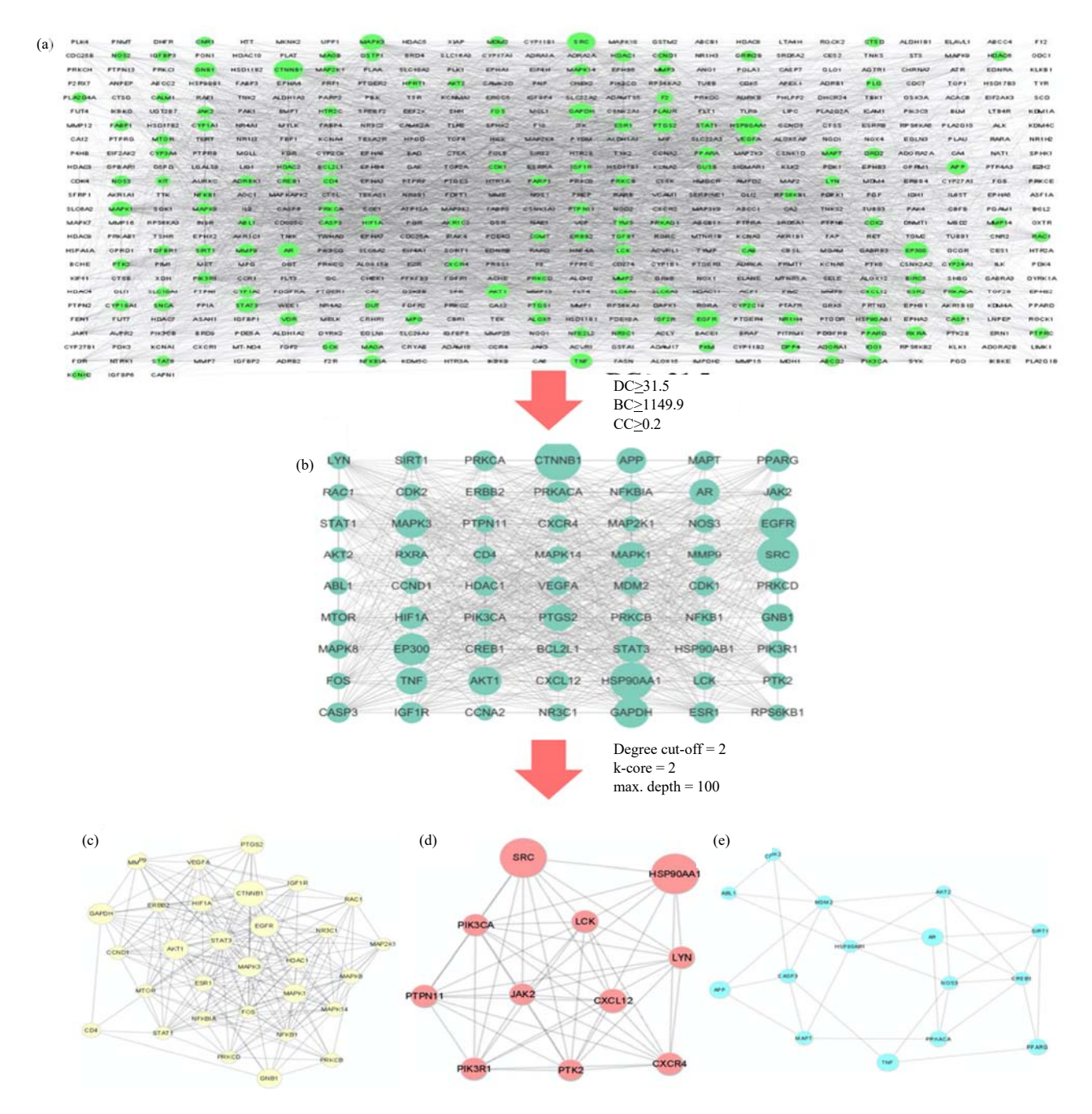


Fig. 2(a-e): Herbs-components-targets network of DO analysis, (a) Common genes between DO and LUAD were analyzed via STRING. Notes whose interaction score of 0.7 were visualised in Cytoscape v3.8.2, (b) Notes were further analyzed by the plugin of CytoNCA. In total, 63 core targets reached the cutoff whose DC 1.5, BC 1149.9 and CC 0.2 and (c-e) Three modules of 63 core targets with degree cutoff 2, k-score 2 and max. depth = 100

methoxyflavanone inhibited osteoclasts differentiation and function via the MAPK pathway<sup>36</sup>. Hydroxyobtustyrene, a cinnamyl phenol, exerted an anti-hypoxia effect on neuronal cells<sup>37</sup>. In the present study, 37 ingredients and 796 targets of DO were obtained, which confirmed its wide pharmacological effects.

Recently, the anticancer effects of DO were frequently demonstrated. Li *et al.*<sup>38</sup> found that 4-methoxydalbergione inhibited tumour growth and reduced tumour size in U87 astroglioma via regulation of cell division, cell cycle, p53, TNF and MAPK signalling pathways. Yun's *et al.*<sup>19</sup> study revealed a flavonoid (4-parvifuran) could inhibit the metastasis and

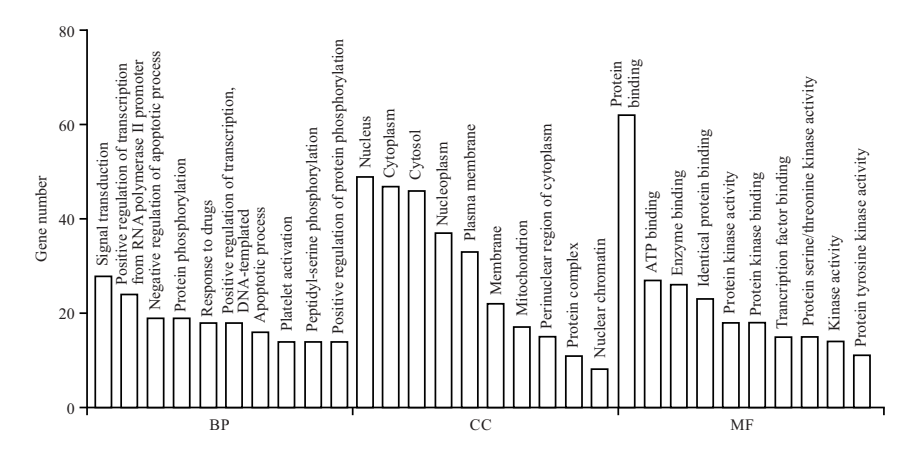


Fig. 3: Top 10 GO enrichment analyses by 63 core targets

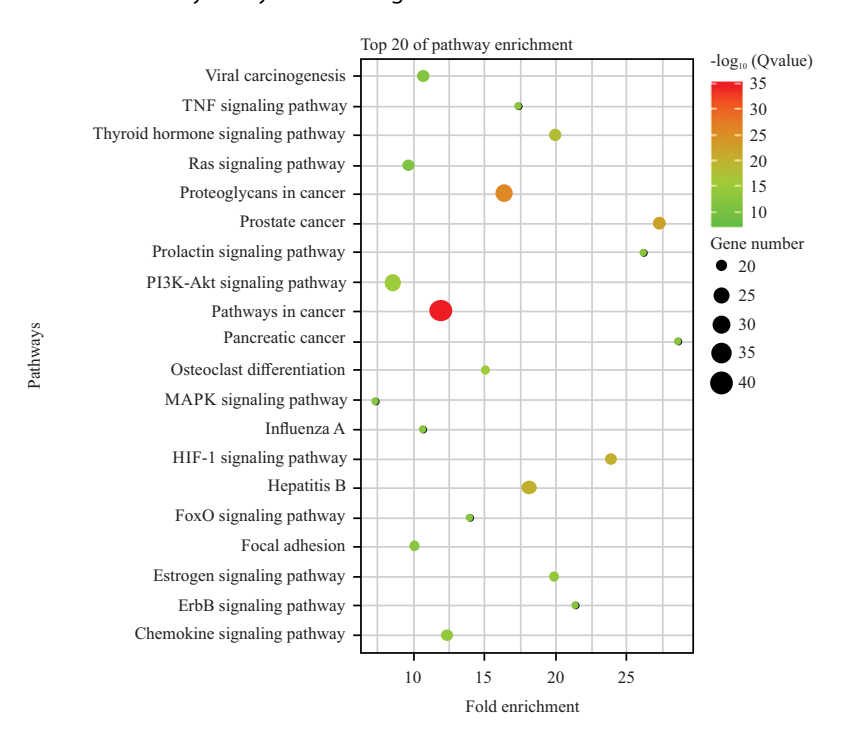


Fig. 4: Top 20 concentrated pathways analyzed from 63 core targets

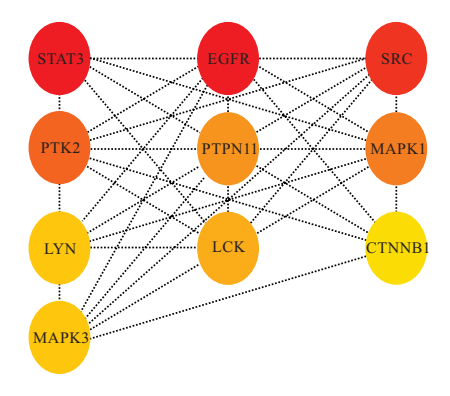


Fig. 5: Top 10 hub genes were explored by Cytoscape 3.8.2 plugin cytoHubba Yellow to red nodes denoted the degree from 57-122

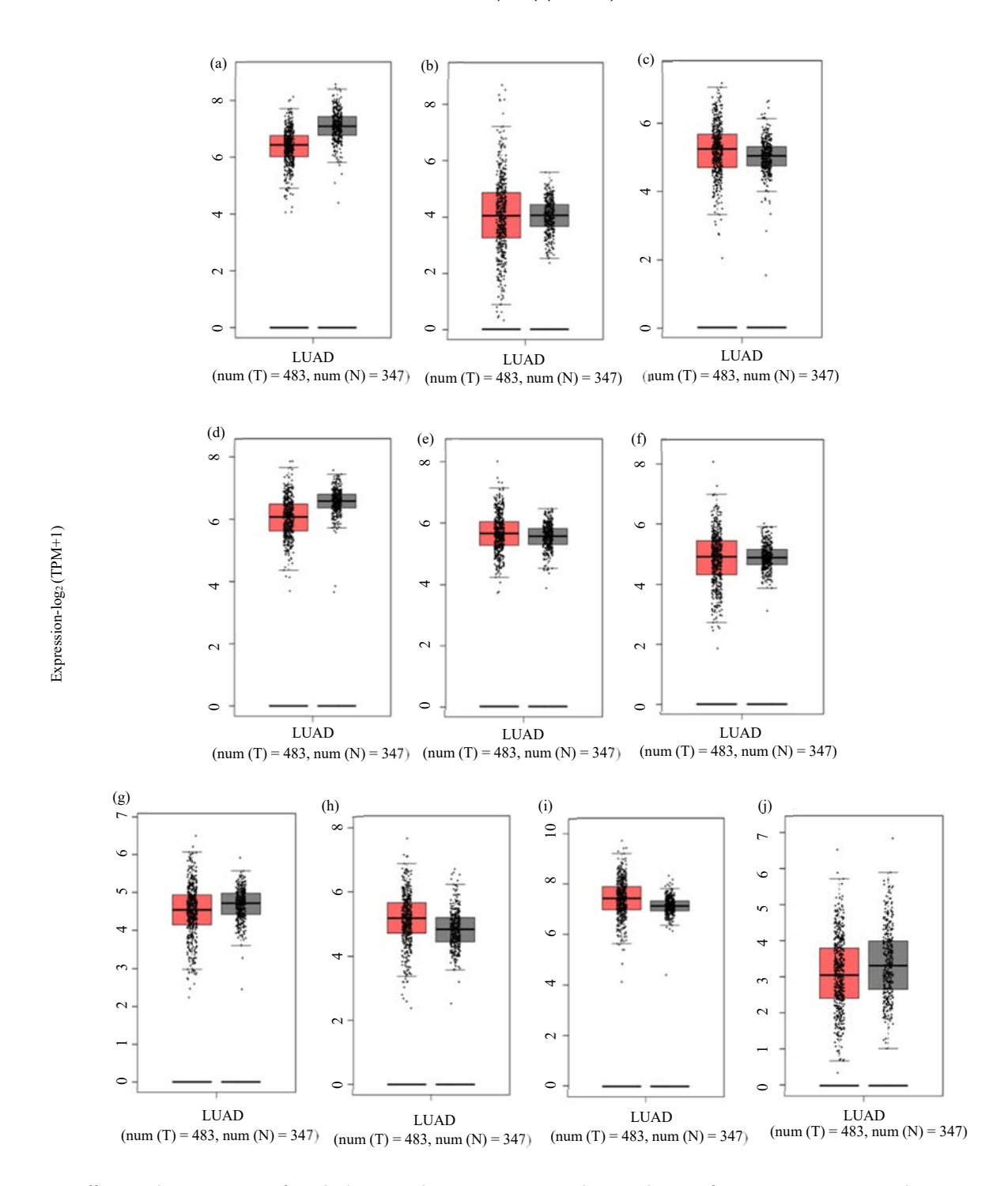


Fig. 6(a-j): Differential expression of 10 hub genes between LUAD and normal tissue from GEPIA, (a) STAT3, (b) EGFR, (c) SRC, (d) MAPK3, (e) PTK2, (f) MAPK1, (g) PTPN11, (h) LYN, (i) CNTTB1 and (j) LCK

metastasis and invasion of osteosarcoma cells through STAT3 and MARKs including JNK, ERK and p38 kinase. Furthermore, cearoin was shown to induce apoptosis in SH-SY5Y neuroblastoma cells through Bcl-2 and caspase-3<sup>20</sup>. In the present study, 627 genes overlapped between DO and LUAD

were demonstrated, dropping a hint that DO may owe the widely anti-LUAD effects.

LUAD is the most prevalent subtype of NSCLC, which is activated by mutation in EGFR, ALK, Kirsten rat sarcoma virus (KRAS), ROS1 and PIK3CA<sup>39</sup>. In this study, we performed PPI

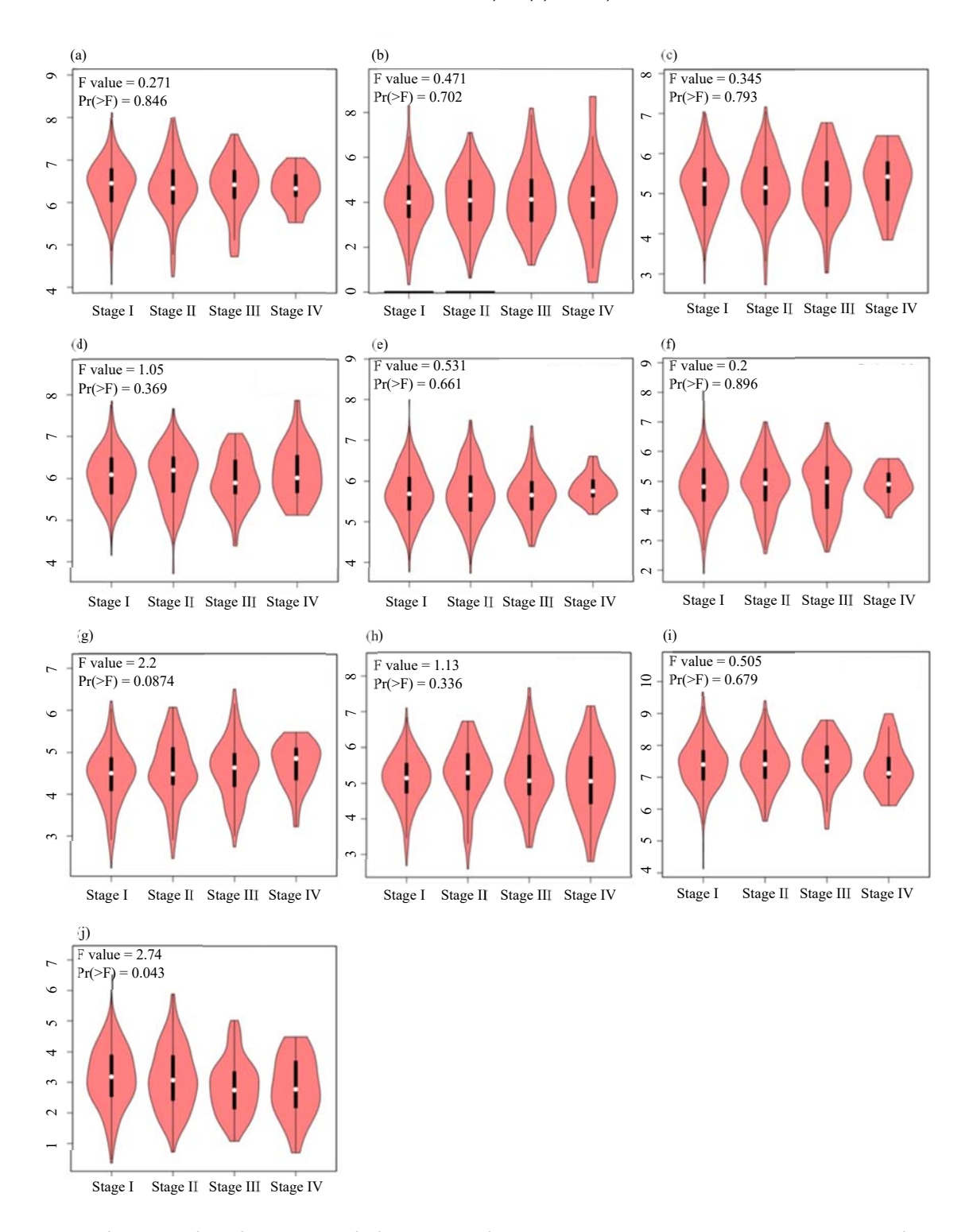


Fig. 7(a-j): Correlation analysis between 10 hub genes and tumour stages in LUAD patients, (a) STAT3, (b) EGFR, (c) SRC, (d) MAPK3, (e) PTK2, (f) MAPK1, (g) PTPN11, (h) LYN, (i) CNTTB1 and (j) LCK

analysis for the 627 overlapping genes and revealed that the LUAD-relative genes EGFR and PIK3CA were clustered in module 1 and module 2, respectively. Those core genes were

enriched in pathways in cancer, proteoglycans pathway and PI3K-AKT signalling pathway, which have been declared in LUAD<sup>40</sup>.

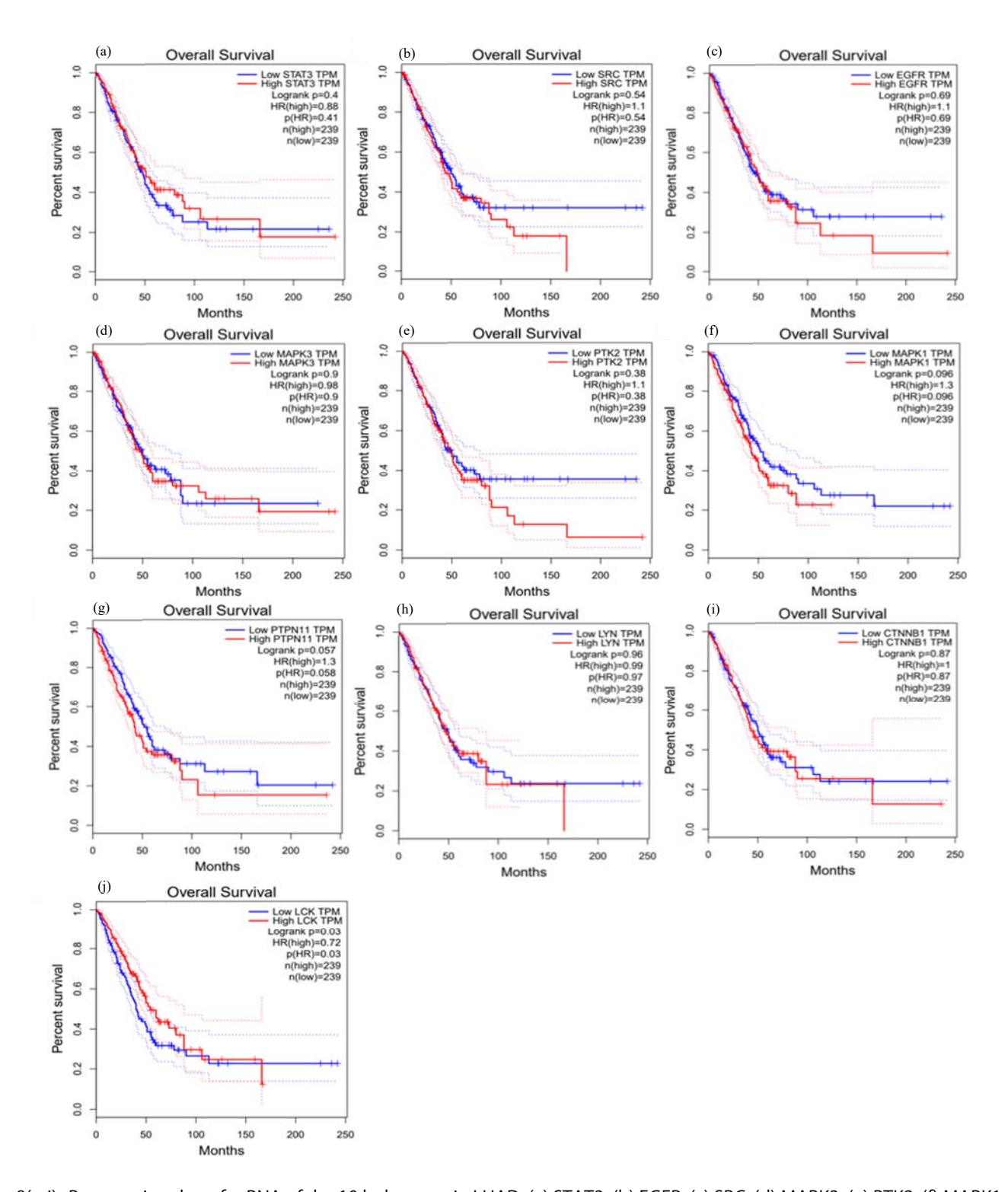


Fig. 8(a-j): Prognostic value of mRNA of the 10 hub genes in LUAD, (a) STAT3, (b) EGFR, (c) SRC, (d) MAPK3, (e) PTK2, (f) MAPK1, (g) PTPN11, (h) LYN, (i) CNTTB1 and (j) LCK

Deregulated host inflammation has been designated as one of the "Hallmarks of Cancer"<sup>41</sup>. Overexpression of checkpoints especially such as T-lymphocyte-associated

protein -4 (CTLA-4) and programmed death-1(PD-1) in T cells negatively regulates T cell activation<sup>42</sup>. The LCK is a tyrosine kinase, which is abundant in lymphoma such as T cells and

involved in several cellular processes including cell cycle control, cell adhesion, cell motility, cell proliferation and cell differentiation through phosphorylating ZAP-70, ITK, protein kinase C and PI3K<sup>43</sup>. It was declared that overexpression of LCK in estrogen-receptor-positive and negative breast cancer samples was associated with better metastasis-free survival<sup>44</sup>. Besides, the prognosis of endometrial cancer and bladder cancer patients with high LCK expression was significantly better than that of the low expression group<sup>45,46</sup>. In the present study, a slightly decreased expression of LCK was demonstrated in LUAD, compared with normal tissue, moreover, LCK expression was negatively correlated to the prognosis stages of LUAD and lower expression of LCK predicted a worse survival rate in LUAD patients. Those results suggested that overexpression of LCK prevented the prognosis of LUAD. Furthermore, as LCK could efficiently phosphorylate PD-147, stimulating an abnormal LCK signal to enhance the rest of the PD-1 blockade may be a new targeted molecular approach for cancer treatment<sup>48</sup>. The current study demonstrated that LCK was the preferential target for 21 compounds from DO, which implied the potential mechanism of the anti-LUAD effect.

# CONCLUSION

DO, as traditional Chinese medicine, shows widespread pharmacological effects including anti-cardiac and anticancer properties. Through network pharmacology analysis, it was illustrated that DO may owe an anti-LUAD effect via modulating the tyrosine kinase LCK and reversing the resistance of chemotherapy. Those results proposed a new role of DO for the treatment of LUAD.

#### SIGNIFICANCE STATEMENT

The present study illustrated that DO may owe an anti-LUAD effect via modulating the tyrosine kinase LCK and reversing chemotherapy resistance by integrating network pharmacology with the GEPIA dataset. Those results proposed a new role of DO for the treatment of LUAD.

# **ACKNOWLEDGMENT**

This work was supported by the Hainan Provincial Natural Science Foundation of China (No. 819QN224, 820QN265), the Scientific cultivation foundation of Hainan Medical University (No. HYPY201909), the Innovation and entrepreneurship

training program for college students (No. S202111810010). Epilepsy Research Science Innovation Group of Hainan Medical University (2022).

# **REFERENCES**

- Cao, W., H.D. Chen, Y.W. Yu, N. Li and W.Q. Chen, 2021. Changing profiles of cancer burden worldwide and in China: A secondary analysis of the global cancer statistics 2020. Chin. Med. J., 134: 783-791.
- Christian, W.J., N.L. Vanderford, J. McDowell, B. Huang and E.B. Durbin *et al.*, 2019. Spatiotemporal analysis of lung cancer histological types in Kentucky, 1995-2014. Cancer Control, Vol. 26. 10.1177/1073274819845873.
- 3. Milano, A.F., 2019. 20-year comparative survival and mortality of cancer of the stomach by age, sex, race, stage, grade, cohort entry time-period, disease duration & selected ICD-O-3 oncologic phenotypes: A systematic review of 157,258 cases for diagnosis years 1973-2014: (SEER\*stat 8.3.4). J. Insur. Med., 48: 5-23.
- 4. Travis, W.D., E. Brambilla, A.G. Nicholson, Y. Yatabe and J.H.M. Austin *et al.*, 2015. The 2015 World Health Organization classification of lung tumors: Impact of genetic, clinical and radiologic advances since the 2004 classification. J. Thoracic Oncol., 10: 1243-1260.
- Lantuejoul, S., L. Fernandez-Cuesta, F. Damiola, N. Girard and A. McLeer, 2020. New molecular classification of large cell neuroendocrine carcinoma and small cell lung carcinoma with potential therapeutic impacts. Transl. Lung Cancer Res., 9: 2233-2244.
- Herbst, R.S., J.V. Heymach and S.M. Lippman, 2008. Lung cancer. New Engl. J. Med., 359: 1367-1380.
- Soria, J.C., Y. Ohe, J. Vansteenkiste, T. Reungwetwattana and B. Chewaskulyong *et al.*, 2018. Osimertinib in untreated EGFRmutated advanced non-small-cell lung cancer. New Engl. J. Med., 378: 113-125.
- 8. Kim, G.T., S.Y. Kim and Y.M. Kim, 2017. Torilis japonica extract fraction compound, EGFR-targeted inhibition of cancer abnormal metastasis in A549 lung cancer cells. Oncol. Rep., 38: 1206-1212.
- 9. Novello, S., J. Mazières, I.J. Oh, J. de Castro and M.R. Migliorino *et al.*, 2018. Alectinib versus chemotherapy in crizotinib-pretreated anaplastic lymphoma kinase (ALK)-positive nonsmall-cell lung cancer: Results from the phase III ALUR study. Ann. Oncol., 29: 1409-1416.
- Park, J., Y. Kobayashi, K.Y. Urayama, H. Yamaura, Y. Yatabe and T. Hida, 2016. Imaging characteristics of driver mutations in EGFR, KRAS, and ALK among treatment-naïve patients with advanced lung adenocarcinoma. PLoS ONE, Vol. 11. 10.1371/journal.pone.0161081.
- 11. Wang, N., L. Wang, X. Meng, J. Wang and L. Zhu *et al.*, 2019. Osimertinib (AZD9291) increases radio-sensitivity in EGFR T790M non-small cell lung cancer. Oncol. Rep., 41: 77-86.

- 12. Wang, S., P. Ma, G. Ma, Z. Lv and F. Wu *et al.*, 2020. Value of serum tumor markers for predicting EGFR mutations and positive ALK expression in 1089 Chinese non-small-cell lung cancer patients: A retrospective analysis. Eur. J. Cancer, 124: 1-14.
- 13. Yang, Y., Y. Yang, X. Zhou, X. Song and M. Liu *et al.*, 2015. EGFR I858R mutation is associated with lung adenocarcinoma patients with dominant ground-glass opacity. Lung Cancer, 87: 272-277.
- 14. Shaw, A.T., G.J. Riely, Y.J. Bang, D.W. Kim and D.R. Camidge *et al.*, 2019. Crizotinib in *ROS1*-rearranged advanced non-small-cell lung cancer (NSCLC): Updated results, including overall survival, from profile 1001. Ann. Oncol., 30: 1121-1126.
- 15. Kris, M.G., L.E. Gaspar, J.E. Chaft, E.B. Kennedy and C.G. Azzoli *et al.*, 2017. Adjuvant systemic therapy and adjuvant radiation therapy for stage I to IIIA completely resected non-small-cell lung cancers: American society of clinical oncology/cancer care ontario clinical practice guideline update. J. Clin. Oncol., 35: 2960-2974.
- van der Wekken, A.J., A. Saber, T.J.N. Hiltermann, K. Kok, A. van den Berg and H.J.M. Groen, 2016. Resistance mechanisms after tyrosine kinase inhibitors afatinib and crizotinib in non-small cell lung cancer, a review of the literature. Crit. Rev. Oncol. Hematol., 100: 107-116.
- 17. Miller, K.D., L. Nogueira, A.B. Mariotto, J.H. Rowland and K.R. Yabroff *et al.*, 2019. Cancer treatment and survivorship statistics, 2019. CA: Cancer J. Clin., 69: 363-385.
- 18. Liu, K., X. Tao, J. Su, F. Li and F. Mu *et al.*, 2021. Network pharmacology and molecular docking reveal the effective substances and active mechanisms of *Dalbergia odoriferain* protecting against ischemic stroke. PLoS ONE, Vol. 16. 10.1371/journal.pone.0255736.
- 19. Yun, H.M., K.R. Park, T.H. Quang, H. Oh, J.T. Hong, Y.C. Kim and E.C. Kim, 2017. 4-parvifuran inhibits metastatic and invasive actions through the JAK2/STAT<sub>3</sub> pathway in osteosarcoma cells. Arch. Pharm. Res., 40: 601-609.
- Bastola, T., R.B. An, Y.C. Kim, J. Kim and J. Seo, 2017. Cearoin induces autophagy, ERK activation and apoptosis via ROS generation in SH-SY5Y neuroblastoma cells. Molecules, Vol. 22. 10.3390/molecules22020242.
- 21. Park, J.H., Y.J. Jang, Y.J. Choi, J.W. Jang and J.H. Kim *et al.*, 2013. Fisetin inhibits matrix metalloproteinases and reduces tumor cell invasiveness and endothelial cell tube formation. Nutr. Cancer, 65: 1192-1199.
- 22. Li, S. and B. Zhang, 2013. Traditional Chinese medicine network pharmacology: Theory, methodology and application. Chin. J. Nat. Med., 11: 110-120.
- 23. Tang, Y., M. Li, J. Wang, Y. Pan and F.X. Wu, 2015. CytoNCA: A cytoscape plugin for centrality analysis and evaluation of protein interaction networks. Biosystems, 127: 67-72.

- 24. Zhao, X., C. Wang, H. Meng, Z. Yu, M. Yang and J. Wei, 2020. *Dalbergia odorifera*: A review of its traditional uses, phytochemistry, pharmacology, and quality control. J. Ethnopharmacol., Vol. 248. 10.1016/j.jep.2019.112328.
- Shang, H., J. Zhang, C. Yao, B. Liu and X. Gao et al., 2013. Qi-shen-yi-qi dripping pills for the secondary prevention of myocardial infarction: A randomised clinical trial. Evidence-Based Complementary Altern. Med., Vol. 2013. 10.1155/2013/738391.
- Lee, C., J.W. Lee, Q. Jin, D.S. Jang and S.J. Lee et al., 2013. Inhibitory constituents of the heartwood of *Dalbergia odorifera* on nitric oxide production in RAW 264.7 macrophages. Bioorgan. Med. Chem. Lett., 23: 4263-4266.
- 27. Lee, S.H., J.Y. Kim, G.S. Seo, Y.C. Kim and D.H. Sohn, 2009. Isoliquiritigenin, from *Dalbergia odorifera*, up-regulates anti-inflammatory heme oxygenase-1 expression in RAW264.7 macrophages. Inflamm. Res., 58: 257-262.
- 28. Lee, D.S., B. Li, N.K. Im, Y.C. Kim and G.S. Jeong, 2013. 4,2,5 -Trihydroxy-4 -methoxychalcone from *Dalbergia odorifera* exhibits anti-inflammatory properties by inducing heme oxygenase-1 in murine macrophages. Int. Immunopharmacol., 16: 114-121.
- 29. Yin, Z., R. Park and B.M. Choi, 2020. Isoparvifuran isolated from *Dalbergia odorifera* attenuates H<sub>2</sub>O<sub>2</sub>-induced senescence of BJ cells through SIRT1 activation and AKT/mTOR pathway inhibition. Biochem. Biophys. Res. Commun., 533: 925-931.
- Lee, D.S. and G.S. Jeong, 2014. Arylbenzofuran isolated from Dalbergia odorifera suppresses lipopolysaccharide-induced mouse BV2 microglial cell activation, which protects mouse hippocampal HT22 cells death from neuroinflammation-mediated toxicity. Eur. J. Pharmacol., 728: 1-8.
- 31. Lin, R., J. Duan, F. Mu, H. Bian and M. Zhao *et al.*, 2018. Cardioprotective effects and underlying mechanism of Radix *Salvia miltiorrhiza* and Lignum *Dalbergia odorifera* in a pig chronic myocardial ischemia model. Int. J. Mol. Med., 42: 2628-2640.
- 32. Lin, R., F. Mu, Y. Li, J. Duan and M. Zhao *et al.*, 2021. *Salvia miltiorrhiza* and the volatile of *Dalbergia odorifera* attenuate chronic myocardial ischemia injury in a pig model: A metabonomic approach for the mechanism study. Oxid. Med. Cell. Longevity, Vol. 2021. 10.1155/2021/8840896.
- Yu, J., W. Zhang, Y. Zhang, Y. Wang, B. Zhang, G. Fan and Y. Zhu, 2017. A critical courier role of volatile oils from *Dalbergia odorifera* for cardiac protection *in vivo* by QiShenYiQi. Sci. Rep., Vol. 7. 10.1038/s41598-017-07659-x.
- 34. Lai, X.X., N. Zhang, L.Y. Chen, Y.Y. Luo, B.Y. Shou, X.X. Xie and R.H. Liu, 2020. Latifolin protects against myocardial infarction by alleviating myocardial inflammatory via the HIF-1α/NF-κB/IL-6 pathway. Pharm. Biol., 58: 1165-1175.
- 35. Lim, S.H., B.S. Li, R.Z. Zhu, J.H. Seo and B.M. Choi, 2020. Latifolin inhibits oxidative stress-induced senescence *via* upregulation of SIRT1 in human dermal fibroblasts. Biol. Pharm. Bull., 43: 1104-1110.

- 36. Im, N.K., J.Y. Choi, H. Oh, Y.C. Kim and G.S. Jeong, 2013. 6,4 -Dihydroxy-7-methoxyflavanone inhibits osteoclast differentiation and function. Biol. Pharm. Bull., 36: 796-801.
- 37. Iwai, T., K. Obara, C. Ito, H. Furukawa and J.I. Oka, 2018. Hydroxyobtustyrene protects neuronal cells from chemical hypoxia-induced cell death. J. Nat. Med., 72: 915-921.
- 38. Li, R., C.Q. Xu, J.X. Shen, Q.Y. Ren and D.L. Chen *et al.*, 2021. 4-Methoxydalbergione is a potent inhibitor of human astroglioma U87 cells *in vitro* and *in vivo*. Acta Pharmacol. Sin., 42: 1507-1515.
- 39. The Cancer Genome Atlas Research Network, 2014. Comprehensive molecular profiling of lung adenocarcinoma. Nature, 511: 543-550.
- 40. Zhu, Z., H. Sun, G. Ma, Z. Wang, E. Li, Y. Liu and Y. Liu, 2012. Bufalin induces lung cancer cell apoptosis via the inhibition of PI3K/AKT pathway. Int. J. Mol. Sci., 13: 2025-2035.
- 41. Schreiber, R.D., L.J. Old and M.J. Smyth, 2011. Cancer immunoediting: Integrating immunity's roles in cancer suppression and promotion. Science, 331: 1565-1570.
- 42. Blackburn, S.D., A. Crawford, H. Shin, A. Polley, G.J. Freeman and E.J. Wherry, 2009. Tissue-specific differences in PD-1 and PD-L1 expression during chronic viral infection: Implications for CD8 T-cell exhaustion. J. Virol., 84: 2078-2089.

- 43. Singh, P.K., A. Kashyap and O. Silakari, 2018. Exploration of the therapeutic aspects of Lck: A kinase target in inflammatory mediated pathological conditions. Biomed. Pharmacother., 108: 1565-1571.
- 44. van Roosmalen, W., S.E.L. Dévédec, O. Golani, M. Smid and I. Pulyakhina *et al.*, 2015. Tumor cell migration screen identifies SRPK1 as breast cancer metastasis determinant. J. Clin. Invest., 125: 1648-1664.
- 45. Ma, J., J.K. Zhang, D. Yang and X.X. Ma, 2020. Identification of novel prognosis-related genes in the endometrial cancer immune microenvironment. Aging, 12: 22152-22173.
- Zhao, X., Y. Tang, H. Ren and Y. Lei, 2020. Identification of prognosis-related genes in bladder cancer microenvironment across TCGA database. BioMed Res. Int., Vol. 2020. 10.1155/2020/9143695.
- 47. Hui, E., J. Cheung, J. Zhu, X. Su and M.J. Taylor *et al.*, 2017. T cell costimulatory receptor CD28 is a primary target for PD-1-mediated inhibition. Science, 355: 1428-1433.
- Gulati, P., J. Rühl, A. Kannan, M. Pircher and P. Schuberth et al., 2018. Aberrant lck signal via CD28 costimulation augments antigen-specific functionality and tumor control by redirected T cells with PD-1 blockade in humanized mice. Clin. Cancer Res., 24: 3981-3993.